

# Reaction Sintering of Aluminium Titanate: I—Effect of MgO Addition

V. Buscaglia,<sup>a</sup> P. Nanni,<sup>b</sup> G. Battilana,<sup>a</sup> G. Aliprandi<sup>c</sup> & C. Carry<sup>d</sup>

<sup>a</sup> Istituto di Chimica Fisica Applicata dei Materiali, C. N. R., via De Marini 6, 16149 Genoa, Italy

<sup>b</sup> Istituto di Chimica, Università di Genova, Fiera del Mare, Piazzale Kennedy, 16129 Genoa, Italy

<sup>c</sup> Istituto di Scienza e Tecnologia per l'Ingegneria Chimica, Viale Causa, 16145 Genoa, Italy

<sup>d</sup> Ecole Polytechnique Fédérale de Lausanne, Département des Matériaux, MX-D Ecublens, 1015 Lausanne, Switzerland

(Received 29 December 1992; revised version received 5 May 1993; accepted 4 December 1993)

## Abstract

The effect of 2 wt% MgO addition on the reactive sintering of  $\text{Al}_2\text{TiO}_5$  was studied starting from commercially available alumina and rutile powders. The formation of titanate, the successive sintering process and the corresponding microstructure evolution have been investigated using differential dilatometry, X-ray powder diffraction and scanning electron microscopy. For pure  $\text{Al}_2\text{TiO}_5$  the reaction occurs initially by a nucleation and rapid growth process and, afterwards, by the slow conversion of unreacted oxide particles by solid-state diffusion. The addition of MgO changes the mechanism of titanate formation, probably by making easy the nucleation of the new phase through the intermediate formation of  $\text{MgAl}_2\text{O}_4$ , followed by the growth of a Mg-rich solid solution. The main result is a strong reduction of the average grain size and remarkable increase of the density of the final material.

Der Effekt der Zugabe von 2 Gew.% MgO auf das reaktive Sintern von  $\text{Al}_2\text{TiO}_5$  wurde, ausgehend von kommerziell erhältlichen Aluminiumoxyd- und Rutilpulvern, untersucht. Die Bildung von Titanat, der fortschreitende Sinterprozeß und das sich ergebende Mikrogefüge wurde mit Hilfe von Differentialdilatometrie, Röntgenpulverbeugung und Rasterelektronenmikroskopie untersucht. Bei reinem  $\text{Al}_2\text{TiO}_5$  beginnt die Reaktion durch Keimbildung und ein schnelles Wachstum, gefolgt von einer Reaktion der noch nicht umgewandelten Oxydteilchen durch Festkörperdiffusion. Die Zugabe von MgO verändert den Bildungsmechanismus des Titanats, wahrscheinlich durch eine Begünstigung der Keimbildung der neuen Phase über die zwischenzeitliche Bildung von  $\text{MgAl}_2\text{O}_4$  und gefolgt von langsamen Wachstum eines Mg-reichen Mischkristalls. Das wichtigste Ergebnis ist eine starke Abnahme der

mittleren Korngröße und ein bemerkenswerter Anstieg der Dichte des Endmaterials.

On a étudié l'effet d'un ajout de 2% pond. de MgO sur le frittage réactionnel d' $\text{Al}_2\text{TiO}_5$  à partir de poudres d'alumine et de rutile de qualité commerciale. La formation du titanate, et l'évolution de la microstructure lors du frittage qui lui est consécutif ont été suivies par dilatométrie différentielle, diffraction X de poudres, et microscopie à balayage. Pour  $\text{Al}_2\text{TiO}_5$  pur, la réaction débute par une nucléation suivie d'une croissance rapide; les particules qui n'ont pas réagi se transforment ensuite lentement par diffusion à l'état solide. L'addition de MgO modifie le mécanisme de formation du titanate. Il semble que la formation du composé intermédiaire  $\text{MgAl}_2\text{O}_4$ , suivie de la croissance d'une solution solide riche en Mg, favorise la nucléation de la nouvelle phase. Le résultat principal est une réduction importante de la taille de grains et une amélioration notable de la densité du produit final.

## 1 Introduction

Aluminium titanate,  $\text{Al}_2\text{TiO}_5$ , is a material with very low thermal expansion coefficient and low thermal conductivity. These properties make it suitable for applications where thermal insulation and thermal shock resistance are required. The possibility of employing this material for components of internal combustion engines (portliners, manifolds, linings of turbochargers etc.) is under test.<sup>1</sup>  $\text{Al}_2\text{TiO}_5$  presents, however, two important problems. The first one is related to the extensive microcracking which results in the low thermal expansion but also in a low strength. As a consequence, composite materials like  $\text{Al}_2\text{TiO}_5$ -mullite,<sup>2</sup>  $\text{Al}_2\text{TiO}_5$ - $\text{ZrO}_2$ ,<sup>3</sup>  $\text{Al}_2\text{TiO}_5$ - $\text{TiZrO}_4$ - $\text{ZrO}_2$ <sup>4</sup>

and  $\text{Al}_2\text{TiO}_5$ -mullite- $\text{ZrO}_2$ <sup>5</sup> have been developed. Alternatively the formation of solid solutions by  $\text{MgO}$ ,  $\text{ZrO}_2$  and  $\text{SiO}_2$  additions<sup>5,6</sup> has been studied: the most beneficial effect is produced by  $\text{MgO}$ . The second problem is due to the thermodynamic instability of  $\text{Al}_2\text{TiO}_5$  below  $1280^\circ\text{C}$ ,<sup>7</sup> resulting in the decomposition of the material to form an  $\text{Al}_2\text{O}_3$ - $\text{TiO}_2$  mixture. This represents a serious limitation for high-temperature applications. The decomposition can be controlled by adding small amounts of thermal stabilizers, including  $\text{SiO}_2$ ,  $\text{ZrO}_2$ ,  $\text{MgO}$ <sup>5,8</sup> and  $\text{Fe}_2\text{O}_3$ ,<sup>9</sup> which form solid solutions. Only  $\text{MgO}$  and  $\text{Fe}_2\text{O}_3$  can offer a reliable phase stability in oxidizing environments, even if  $\text{Fe}^{3+}$  substitution seems to be less stable against reducing atmospheres. In the present study,  $\text{Al}_2\text{TiO}_5$  and  $\text{Al}_2\text{TiO}_5$  with  $\text{MgO}$  addition were reaction sintered, starting from alumina and rutile. The aim of this work is to clarify the role of  $\text{MgO}$  on the formation reaction of  $\text{Al}_2\text{TiO}_5$  and on the microstructure evolution which leads to the final material.

## 2 Experimental Procedure

Equimolar mixtures of alumina (Keramont 100PCT/TLV/TWA,  $\alpha$ -phase, 99.99%,  $X_{50} = 0.5 \mu\text{m}$ ) and  $\text{TiO}_2$  (Aldrich 1317-80-2, predominantly rutile, 99.9%,  $X_{50} = 1 \mu\text{m}$ ) were mixed and wet-milled in water for 100 h using alumina balls and PE bottles. The resulting powders, after drying and sieving, were isostatically pressed at 150 MPa forming cylinders of  $\approx 10$  mm diameter and  $\approx 100$  mm length. The material containing  $\text{MgO}$  was prepared in the same way by adding 2 wt%  $\text{MgO}$  (Aldrich, 99%). For the sake of brevity, the specimens will be indicated as K when prepared from  $\text{Al}_2\text{O}_3$  and  $\text{TiO}_2$  and as KM for the corresponding ones prepared with  $\text{MgO}$  addition. The reactive and sintering behaviour of the specimens was studied to  $1600^\circ\text{C}$ , with a heating rate of  $1^\circ\text{C}/\text{min}$ , using a differential dilatometer (Setaram DHT) and recording the expansion percentage and the expansion rate of both the specimen and of a reference of known thermal expansion coefficient. The corresponding density and densification rate were then calculated using the green density as initial reference value. To investigate the influence of  $\text{MgO}$  on the formation reaction of  $\text{Al}_2\text{TiO}_5$ , KM specimens were heated to 1100, 1150, 1200, 1300 and  $1450^\circ\text{C}$  at  $1^\circ\text{C}/\text{min}$  and then cooled rapidly. The phases present were determined by X-ray diffraction after grinding (Philips PW1050/PW1729/PW1710). Sintering experiments were performed in a box furnace, heating the samples at  $50^\circ\text{C}/\text{h}$  to the sintering temperature of  $1550^\circ\text{C}$  and then

firing for times up to 24 h in air. An isothermal treatment of 10 h at  $300^\circ\text{C}$  during heating allowed the removal of the organic binder (polysaccharide). The microstructure was observed by SEM (Philips 515), after infiltration of the specimens in epoxy resin and metallographic preparation. The backscatter (BS) mode was especially useful in detecting the presence of unreacted particles. With such a technique,  $\text{TiO}_2$  appears white,  $\text{Al}_2\text{O}_3$  dark grey and  $\text{Al}_2\text{TiO}_5$  of an intermediate grey shade.

## 3 Results

### 3.1 Densification

The density ( $\text{g}/\text{cm}^3$ ) and the densification rate ( $\text{g}/(\text{cm}^3 \text{ min})$ ) versus temperature for pure  $\text{Al}_2\text{TiO}_5$  specimens is presented in Fig. 1(a) (the theoretical density of  $\text{Al}_2\text{TiO}_5$  is  $3.7 \text{ g}/\text{cm}^3$ ). Three different, consecutive, processes can be identified:

- (i) Initial contraction due to the densification of the starting oxide mixture;
- (ii) expansion as a consequence of  $\text{Al}_2\text{TiO}_5$  formation;
- (iii) second contraction due to  $\text{Al}_2\text{TiO}_5$  sintering.

The sintering of the  $\text{Al}_2\text{O}_3/\text{TiO}_2$  matrix (initial green density  $\approx 1.9 \text{ g}/\text{cm}^3$ ) starts at  $\approx 1000^\circ\text{C}$  and stops at  $\approx 1330^\circ\text{C}$ ,  $50^\circ\text{C}$  above the reported forma-

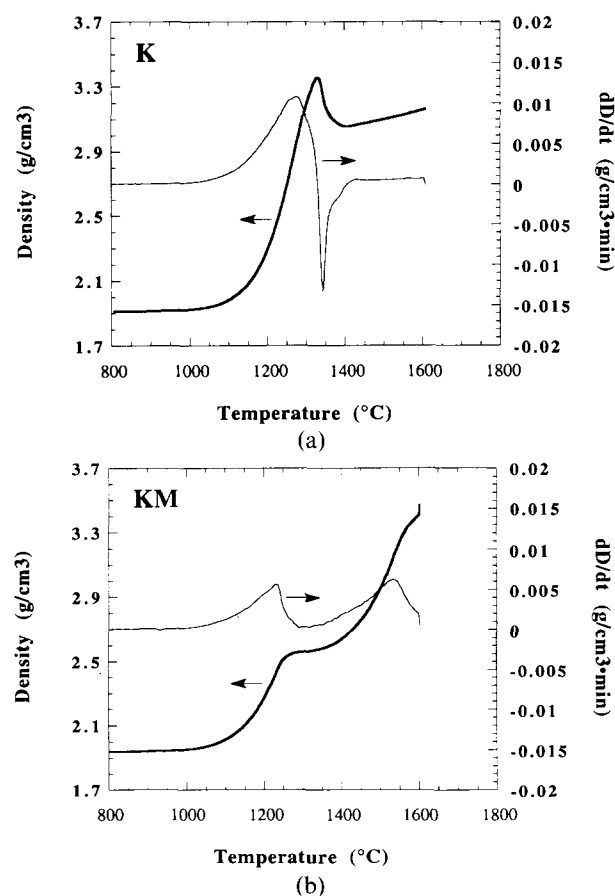


Fig. 1. Density ( $\text{g}/\text{cm}^3$ ) and densification rate ( $\text{g}/(\text{cm}^3 \cdot \text{min})$ ) versus temperature. Heating rate  $1^\circ\text{C}/\text{min}$ . (a) K; (b) KM.

tion temperature of  $\text{Al}_2\text{TiO}_5$  ( $1280^\circ\text{C}^7$ ), corresponding to the maximum of the density curve. The density at the maximum is  $\approx 3.3 \text{ g/cm}^3$ . The shrinkage (16.5%) is more than twice as high as that observed for the corresponding pure alumina without rutile (6.8%) at the same temperature, but close to that of pure rutile ( $\approx 15\%$ ). The accelerated densification has been explained in terms of the greater diffusion coefficient of Al ions in  $\text{TiO}_2$  in comparison to Al ions in  $\text{Al}_2\text{O}_3$  and Ostwald ripening of the alumina grains.<sup>10</sup> The position of the maximum of the density curve corresponds to the temperature at which the expansion related to the  $\text{Al}_2\text{TiO}_5$  formation offsets the matrix densification. The lower density of the titanate ( $3.7 \text{ g/cm}^3$ ) in comparison with the equimolar  $\text{Al}_2\text{O}_3/\text{TiO}_2$  mixture ( $4.1 \text{ g/cm}^3$ ) is responsible for the volume increase and the expansion rate is related to the  $\text{Al}_2\text{TiO}_5$  formation rate. Two minima are present on the densification rate curve: the first one, sharp, at  $\approx 1345^\circ\text{C}$ , and a second one, less pronounced, at  $\approx 1380^\circ\text{C}$ . This can be interpreted in terms of two different reaction mechanisms, as will be discussed later. A second shrinkage starts at  $\approx 1410^\circ\text{C}$ , corresponding to the sintering of the titanate; however, the densification rate is very low and limited densification occurs. As a consequence the final density will be mainly related to the initial green density and to the sintering level of the oxides matrix.

The addition of MgO has two main important effects:

- Eliminates the expansion process related to titanate formation and lowers the temperature at which the sintering of  $\text{Al}_2\text{TiO}_5$  starts.
- Lowers the titanate formation temperature reducing the densification of the starting oxides mixture.

These effects can be observed on the density curve of Fig. 1(b). After the initial densification of the unreacted matrix (initial green density  $\approx 1.9 \text{ g/cm}^3$ ), the formation of titanate will occur at a reduced rate in comparison with K specimens and will start at a lower temperature, 1230 as against  $1255^\circ\text{C}$  (the position of the maximum of the densification rate can be approximated to the titanate formation temperature). At  $\approx 1300^\circ\text{C}$ , densification of the forming titanate starts, avoiding further expansion of the specimen.

### 3.2. Formation of intermediate phases

The phases detected by X-ray diffraction on KM specimens heated at different temperatures were:  $\alpha\text{-Al}_2\text{O}_3$ , rutile and  $\text{MgAl}_2\text{O}_4$  (spinel) at 1100 and  $1150^\circ\text{C}$ ;  $\alpha\text{-Al}_2\text{O}_3$ , rutile,  $\text{MgAl}_2\text{O}_4$  and  $\text{Al}_{2(1-x)}$

$\text{Mg}_x\text{Ti}_{(1+x)}\text{O}_5$  with  $x \approx 0.25$  at  $1200^\circ\text{C}$ ;  $\alpha\text{-Al}_2\text{O}_3$ , rutile (traces) and  $\text{Al}_{2(1-x)}\text{Mg}_x\text{Ti}_{(1+x)}\text{O}_5$  with  $x \approx 0.1$  at  $1300^\circ\text{C}$ . The calculation of  $x$  was carried out from the cell constants determined by X-ray diffraction, assuming a linear dependence from composition, as previously reported.<sup>8</sup> At higher temperatures only  $\alpha\text{-Al}_2\text{O}_3$  and solid solution were detected. Even though no quantitative X-ray diffraction analysis has been performed, the comparison between the reflection intensities shows that the amount of  $\text{MgAl}_2\text{O}_4$  is almost constant at 1100 and  $1150^\circ\text{C}$ , but is strongly reduced at  $1200^\circ\text{C}$ . Formation of magnesium titanates ( $\text{Mg}_2\text{TiO}_4$ ,  $\text{MgTiO}_3$  and  $\text{MgTi}_2\text{O}_5$ ) was not detected within the limits of X-ray diffraction.

### 3.3 Microstructure

Since in both cases the experiments have been carried out starting from an equimolar  $\text{Al}_2\text{O}_3\text{--TiO}_2$  mixture, and the formation of the solid solutions occurs by substitution of 2  $\text{Al}^{3+}$  by 1  $\text{Mg}^{2+}$  and 1  $\text{Ti}^{4+}$ ,<sup>8</sup> the specimens with MgO addition lead to the ultimate formation of  $\text{Al}_{2(1-x)}\text{Mg}_x\text{Ti}_{(1+x)}\text{O}_5$ , with  $x = 0.099$  (theoretical) and contain an excess of  $\text{Al}_2\text{O}_3$  (9.89 wt%), which forms a second phase in the sintered materials. Considering the accuracy of the diffraction method, the obtained values of  $x$  are consistent with the expected result, indicating that Mg completely enters in the solid solution. The comparison of microstructure corresponding to some characteristic temperatures of the densification curves is useful to clarify the effect of MgO addition. Figures 2(a) (K) and 3(a) (KM) show the microstructure at a temperature corresponding to the maximum of the densification rate curve ( $1255^\circ\text{C}$  for K,  $1230^\circ\text{C}$  for KM), i.e. the beginning of titanate formation. Large, isolated  $\text{Al}_2\text{TiO}_5$  cells are present on the K specimen whereas they are lacking on the KM specimen, even though solid solution is being formed. The microstructure at the temperature corresponding to the first minimum of the densification rate ( $1345^\circ\text{C}$  for K,  $1295^\circ\text{C}$  for KM), i.e. the maximum titanate formation rate, is presented in Figs 2(b) (K) and 3(b) (KM). The K specimen presents at this stage large titanate cells which have grown up to impinge onto each other but contain a large number of  $\text{Al}_2\text{O}_3$  and  $\text{TiO}_2$  small inclusions. In contrast, the KM specimen presents a fine-grained, partially reacted structure. Figures 2(c) (K) and 3(c) (KM) show the microstructure corresponding to  $1450^\circ\text{C}$ . For the K specimen, the conversion is still incomplete, as many particles of  $\text{TiO}_2$  and  $\text{Al}_2\text{O}_3$  are present. In contrast, the KM specimen is completely reacted and the sintering process is in progress. At  $1550^\circ\text{C}$ , the reaction is almost complete in the K specimen (Fig. 2(d)), only few  $\text{TiO}_2$

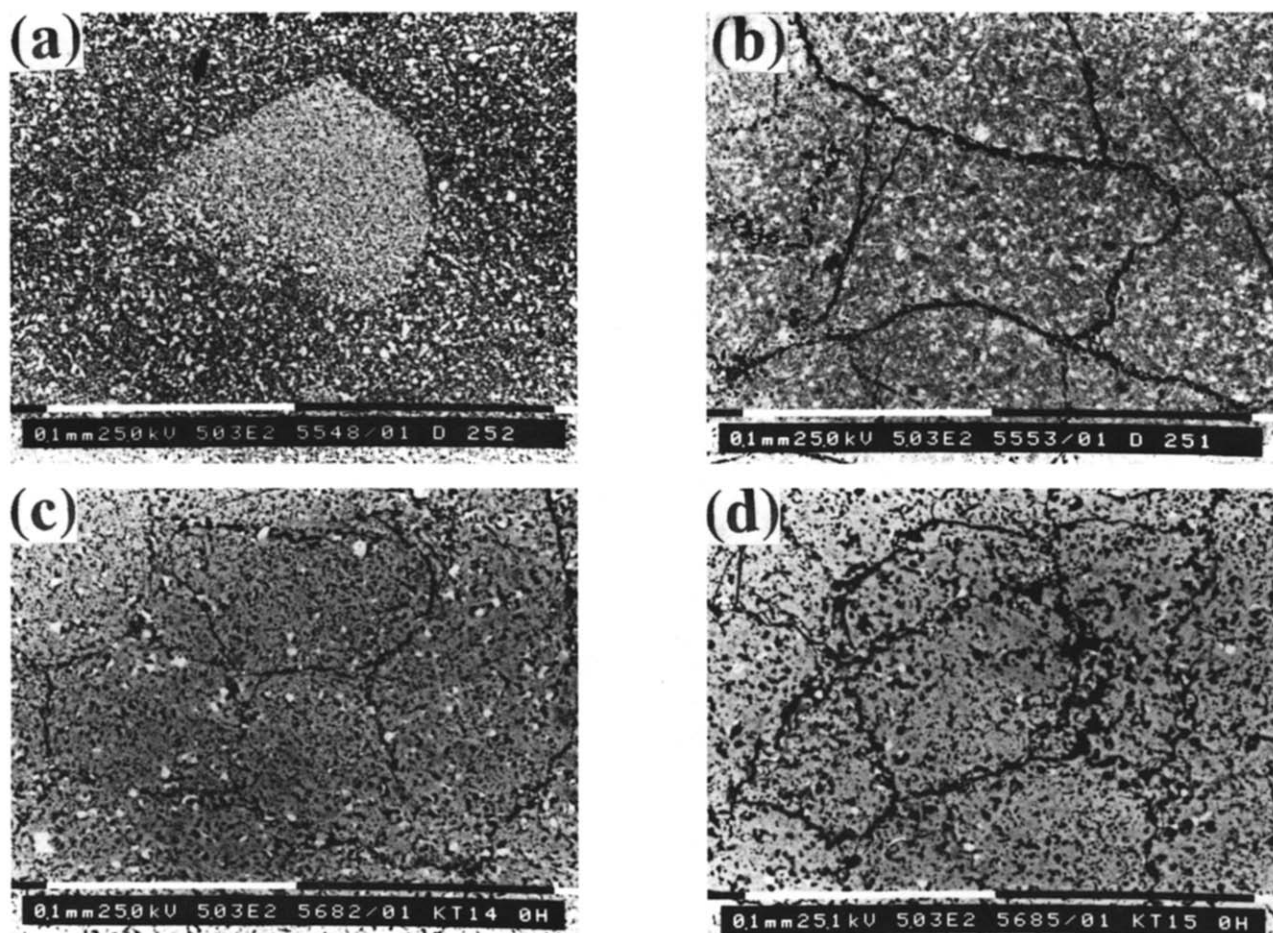


Fig. 2. Microstructure (BEI images) of K specimen versus temperature heating at 1°C/min. (a) 1255°C; (b) 1345°C; (c) 1450°C (d) 1550°C.

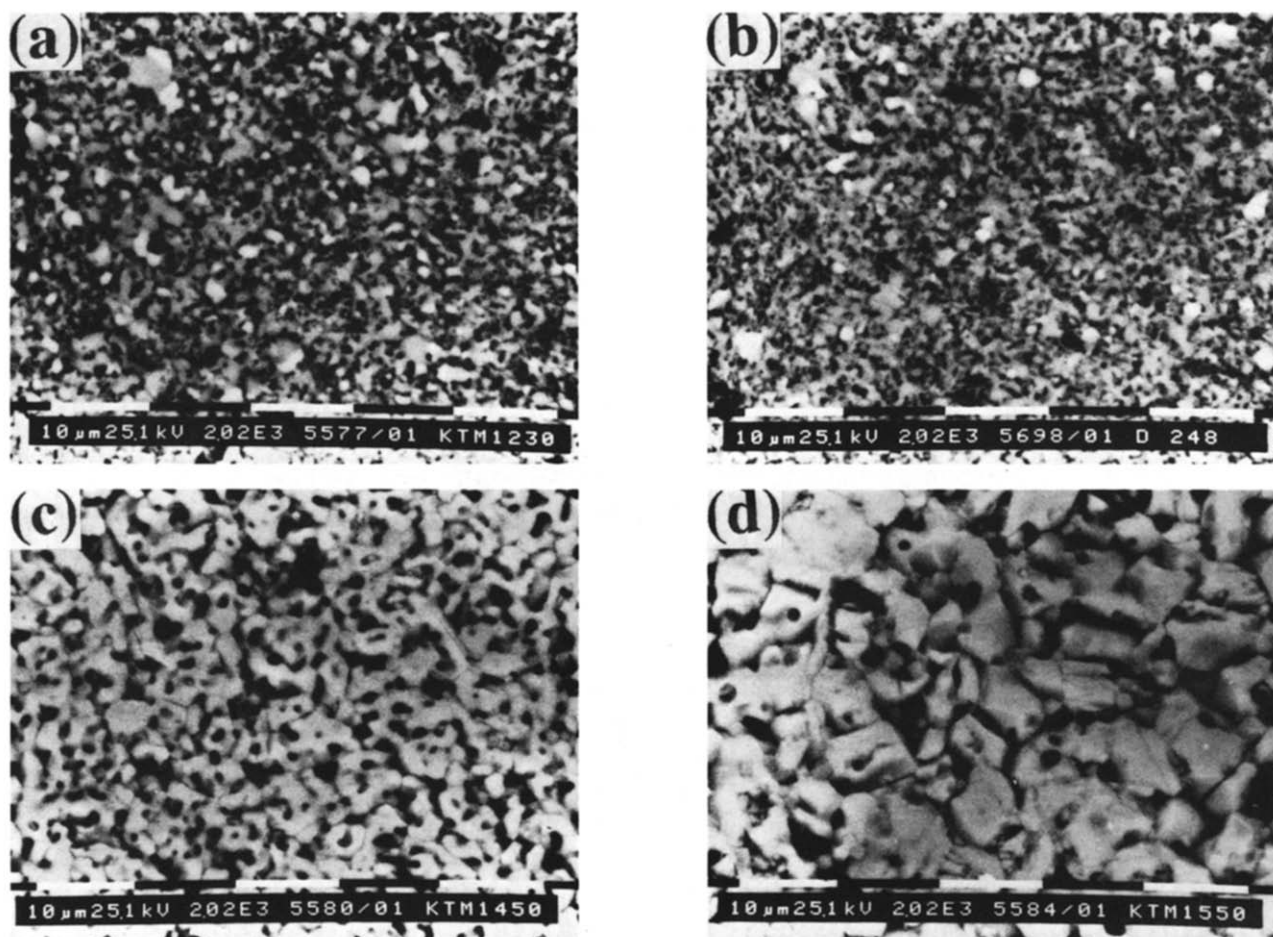


Fig. 3. Microstructure (BEI images) of KM specimen versus temperature heating at 1°C/min. (a) 1230°C; (b) 1295°C; (c) 1450°C (d) 1550°C.

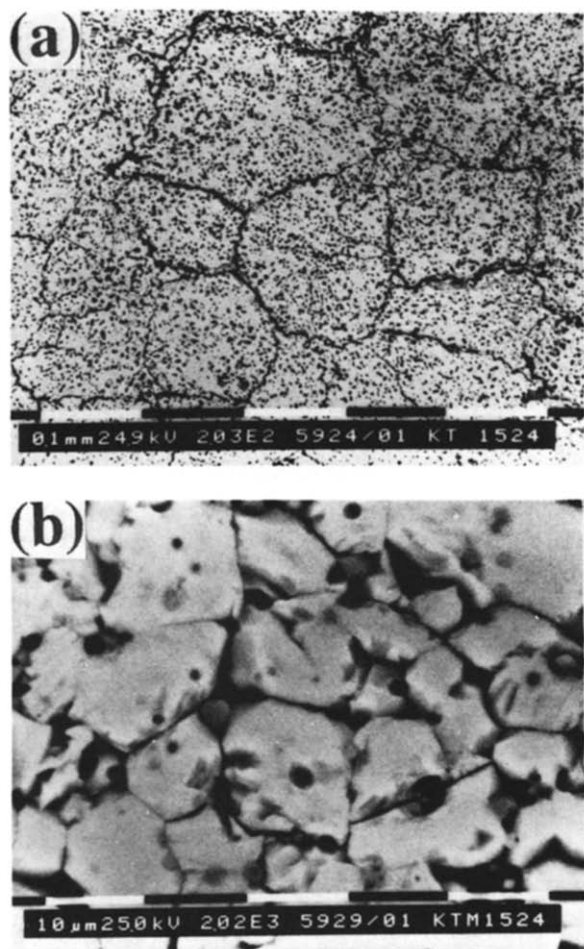


Fig. 4. Microstructure (BEI images) of (a) K and (b) KM specimen after 24 h sintering at 1550°C.

particles are visible; the general microstructure is unchanged in comparison to that at 1450°C. The KM specimen shows a remarkable microstructure evolution with strong increase of density and grain growth (Fig. 3(d)). Prolonged sintering of K specimens at 1550°C does not affect the final microstructure, as shown in Fig. 4(a) for 24 h isothermal treatment. The density of the sintered body, measured with a water-immersion method, is  $\approx 2.8 \text{ g/cm}^3$  (76% of the theoretical density) and the average grain size, expressed as mean intercept length, is  $\approx 200 \mu\text{m}$ . KM specimens, sintered in the same conditions, develop a two-phase microstructure with finer grains, as shown in Fig. 4(b). The dark particles consist of  $\text{Al}_2\text{O}_3$  and are often located at three-grain joints and are related to the excess of alumina present in the starting mixture, as already reported. The titanate grains are equiaxed with average size (mean intercept length) of  $\approx 13 \mu\text{m}$ . The density of the sintered body is  $\approx 3.45 \text{ g/cm}^3$  (93% of the theoretical density). In conclusion, specimens of pure  $\text{Al}_2\text{TiO}_5$  develop large grains with extensive intra- and intergranular porosity; in contrast, the formation of the solid solution results in a dramatic reduction of the grain size and a final higher density.

#### 4 Discussion

The formation of  $\text{Al}_2\text{TiO}_5$  by solid-state reaction between  $\text{Al}_2\text{O}_3$  and  $\text{TiO}_2$  powders of different granulometry has been carefully investigated.<sup>10–12</sup> Depending on temperature, different overall reaction kinetics and microstructure evolution have been observed. In the range 1280–1400°C, the chemical driving force (proportional to the difference between the  $\text{Al}_2\text{TiO}_5$  formation temperature, 1280°C, and the experimental temperature) is too small in comparison with the strain energy associated to bulk nucleation. As a consequence, titanate growth can start only at a limited number of 'easy to nucleate' sites, following the Avrami kinetic law. The rapid transport of Al ions through  $\text{TiO}_2$  results in high growth rates. At  $T > 1400^\circ\text{C}$ , a large number of nucleation sites is available and the reactants are quasi-immediately separated by the forming titanate, resulting in a low growth rate controlled by solid-state diffusion through the  $\text{Al}_2\text{TiO}_5$  layer. The two minima of the densification rate curves for specimens without MgO addition can be related to the two different mechanisms. The first minimum is located at 1345°C and can be ascribed to the nucleation–growth process. During this stage, even in the case where the  $\text{Al}_2\text{TiO}_5$  cells grow enough to occupy the entire sample volume, the conversion is only partial and many inclusions of  $\text{Al}_2\text{O}_3$  and  $\text{TiO}_2$  are still present (Fig. 2(a) and (b)). The second minimum occurs at  $\approx 1385^\circ\text{C}$  and can be ascribed to the conversion of the unreacted oxide particles trapped in the titanate grains, which is controlled by solid-state diffusion through the  $\text{Al}_2\text{TiO}_5$  layer (Fig. 3(c)). These conclusions are valid only at the present value of the heating rate or at a lower one; operating with higher heating rates will result in the inhibition of the initial rapid growth process, obtaining smaller grains.<sup>13</sup>

The addition of MgO results in a different titanate formation mechanism. Initially MgO reacts with  $\text{Al}_2\text{O}_3$  to form spinel:



This reaction takes place below 1100°C and determines the complete conversion of MgO. Formation of  $\text{MgTi}_2\text{O}_5$  from MgO and  $\text{TiO}_2$ , even though  $\text{MgTi}_2\text{O}_5$  is more stable than  $\text{Al}_2\text{TiO}_5$ , does not occur, as the standard Gibbs' free energy  $\Delta G^\circ$  of this process is less negative than that corresponding to reaction (1).<sup>10,14</sup> The same conclusion is also valid for  $\text{MgTiO}_3$  and  $\text{Mg}_2\text{TiO}_4$ . For example, at 1000°C, the values of  $\Delta G^\circ$  (J/mol) of formation from the corresponding oxides is  $-33500$  for  $\text{MgAl}_2\text{O}_4$ ,  $-28440$  for  $\text{Mg}_2\text{TiO}_4$ ,  $-22530$  for  $\text{MgTiO}_3$  and  $-25110$  for  $\text{MgTi}_2\text{O}_5$ . As pointed out

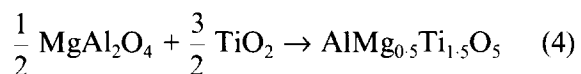
from dilatometry, microstructure and X-ray diffraction, formation of the solid solutions  $\text{Al}_{2(1-x)}\text{Mg}_x\text{Ti}_{(1+x)}\text{O}_5$  takes place at lower temperature in comparison to pure  $\text{Al}_2\text{TiO}_5$  and the value of  $x$  increases as the temperature decreases. Even though  $\text{Al}_2\text{TiO}_5$  is not stable as a pure phase below  $1280^\circ\text{C}$ , it can form at lower temperatures according to



where the square brackets denotes the existence of  $\text{Al}_2\text{TiO}_5$  at activity less than one, i.e. in solid solution. At any temperature  $T < 1280^\circ\text{C}$ , the equilibrium activity of  $\text{Al}_2\text{TiO}_5$  is

$$a(\text{Al}_2\text{TiO}_5) = \exp(-\Delta G^\circ_2/RT) \quad (3)$$

where  $\Delta G^\circ_2$  is the Gibbs' standard free energy of reaction (2) and  $\text{Al}_2\text{O}_3$  and  $\text{TiO}_2$  have been considered as phases at unit activity. Considering that there is not a solubility limit in the system  $\text{Al}_2\text{TiO}_5$ - $\text{MgTi}_2\text{O}_5$ ,<sup>8</sup>  $a(\text{Al}_2\text{TiO}_5)$  can reasonably be expected to be a monotonically decreasing function of the molar fraction  $x$  of  $\text{MgTi}_2\text{O}_5$ . Since  $\Delta G^\circ_2 = -10.9(T - 1553)$  (J/mol),<sup>11</sup> the equilibrium value of  $x$  will increase as temperature decreases, i.e. a higher amount of MgO is required for titanate stability. As a consequence, titanate formation it is likely to begin according to:



at some temperature between  $1150$  and  $1200^\circ\text{C}$ . The volume increase for reaction (4) is  $7\text{--}8\%$ , in contrast to  $10\text{--}11\%$  for direct formation of  $\text{Al}_2\text{TiO}_5$  from  $\text{Al}_2\text{O}_3$  and  $\text{TiO}_2$ , with easier nucleation of the new phase. As temperature increases, the solid solution becomes progressively diluted in Mg by reaction with the excess of  $\text{Al}_2\text{O}_3$  and  $\text{TiO}_2$  and the composition parameter  $x$  will gradually approach the final value of  $0.1$ , obeying eqn (3). The Mg-rich titanate crystals initially formed act therefore as preferential sites for further titanate nucleation and growth. The total free energy change for particle nucleation is:

$$\Delta G = \Delta G_c + \Delta G_s + \Delta G_m \quad (5)$$

where  $\Delta G_c$  is the contribution from the reaction,  $\Delta G_s$  the contribution from interfacial energy and  $\Delta G_m$  the contribution from strain energy. Both the interfacial energy and the chemical driving force can be affected by the existence of the titanate nuclei. The similar lattice constants of  $\text{MgTi}_2\text{O}_5$  and  $\text{Al}_2\text{TiO}_5$  and their ability to form a solid solution over the total composition range should minimize the contribution arising from the interfacial energy by formation of coherent interfaces and heteroepitaxial growth. On the other hand,

for  $T > 1280^\circ\text{C}$ , the chemical driving force is greater than that for  $\text{Al}_2\text{TiO}_5$  formation, due to the higher thermodynamic stability of the solid solution. As a consequence, further nucleation of the new phase is easier and the reaction will be controlled by solid-state diffusion.

The final grain size will then be mainly determined by density and size of the spinel nuclei and, afterwards, by the process of grain growth during sintering of the titanate. The addition of  $\text{MgTi}_2\text{O}_5$  seed crystals to  $\text{Al}_2\text{TiO}_5$  gel has recently been demonstrated<sup>15</sup> to facilitate lowering of the crystallization temperature and to enhance densification during sintering. Direct seeding of  $\text{Al}_2\text{O}_3$  and  $\text{TiO}_2$  mixtures and perhaps of  $\text{Al}_2\text{TiO}_5$  powders with  $\text{MgAl}_2\text{O}_4$  crystals could be a new route to control the grain size and enhance densification of aluminium titanate-based materials prepared using the traditional ceramic process. However, further work is required to study the effect of added spinel seeds on the final microstructure.

## 5 Conclusions

Reactive sintering of  $\text{Al}_2\text{TiO}_5$  and of a  $\text{Al}_2\text{TiO}_5$ - $\text{MgTi}_2\text{O}_5$  solid solution has been studied starting from alumina and rutile powders. The application of dilatometric techniques allowed the observation of different stages during titanate formation and sintering. Formation of pure  $\text{Al}_2\text{TiO}_5$  initially occurs by a nucleation and rapid growth process and, afterwards, by the slow conversion of unreacted oxides controlled by solid-state diffusion. The addition of MgO make the nucleation of the new phase easy, through the initial formation of  $\text{MgAl}_2\text{O}_4$  followed by the growth of Mg-rich titanate solid-solution particles. As a consequence, the final microstructure is mainly controlled by the density and size of the spinel nuclei and, afterwards, by the process of titanate grain growth, resulting in a strong reduction of the titanate grain size and in a remarkable increase of the final density.

## References

1. Stingl, P., Heinrich, J. & Huber, J., Properties and applications of aluminum titanate components. In *Proceedings of the 2nd International Symposium on Ceramic Materials and Components for Engines*, Lübeck-Travemünde, Germany, April 1986, ed. W. Bunk & H. Hausner. DKG, Bad Honnef, 1986, pp. 369–80.
2. Morishima, H. *et al.*, Synthesis of aluminium titanate-mullite composite having high thermal shock resistance. *J. Mat. Sci. Lett.*, **6** (1987) 389–90.
3. Thomas, H. A. J., Stevens, R. & Gilbert, E., Effect of zirconia additions on the reaction sintering of aluminium titanate. *J. Mat. Sci.*, **26** (1991) 3613–16.



4. Parker, F. J.,  $\text{Al}_2\text{TiO}_5\text{--ZrTiO}_4\text{--ZrO}_2$  composites: a new family of low-thermal-expansion ceramics. *J. Am. Cer. Soc.*, **73** (1990) 929–32.
5. Wohlfromm, H., Moya, J. S. & Peña, P., Effect of  $\text{ZrSiO}_4$  and MgO addition on reaction sintering and properties of  $\text{Al}_2\text{TiO}_5$ -based materials. *J. Mat. Sci.*, **25** (1990) 3753–63.
6. Thomas, H. A. J. & Stevens, R., Aluminium titanate—a literature review. Part 2: Engineering properties and thermal stability. *Brit. Ceram. Trans. J.*, **88** (1989) 184–190.
7. Kato, E., Daimon, K. & Takahashi, J., Decomposition temperature of  $\beta\text{-Al}_2\text{TiO}_5$ . *J. Am. Ceram. Soc.*, **63** (1980) 355–6.
8. Ishitsuka, M., Sato, T., Endo, T. & Shimada, M., Synthesis and thermal stability of aluminum titanate solid solutions. *J. Am. Ceram. Soc.*, **70** (1987) 69–71.
9. Tilloca, G., Thermal stabilization of aluminum titanate and properties of aluminum titanate solid solutions. *J. Mat. Sci.*, **26** (1991) 2809–14.
10. Freudenberg, B., Etude de la réaction à l'état solide  $\text{Al}_2\text{O}_3 + \text{TiO}_2 \rightarrow \text{Al}_2\text{TiO}_5$ . Observation des micro-structures, PhD Thesis, 709, 1987, Ecole Polytechnique Fédérale de Lausanne, Lausanne, Switzerland.
11. Freudenberg, B. & Mocellin, A., Aluminum titanate formation by solid-state reaction of fine  $\text{Al}_2\text{O}_3$  and  $\text{TiO}_2$  powders. *J. Am. Ceram. Soc.*, **70** (1987) 33–38.
12. Freudenberg, B. & Mocellin, A., Aluminum titanate formation by solid-state reaction of coarse  $\text{Al}_2\text{O}_3$  and  $\text{TiO}_2$  powders. *J. Am. Ceram. Soc.*, **71** (1988) 22–28.
13. Buscaglia, V., Bottino, C., Nanni, P., Aliprandi, G. & Carry, C., The effect of MgO on the reactive sintering of  $\text{Al}_2\text{TiO}_5$  starting from a commercial alumina. In *Proceedings of Engineering Ceramics '92*, Smolenice, Czechoslovakia, October 1992, ed. M. Haviar. Reprint, Bratislava, 1993, pp. 192–8.
14. Knacke, O., Kubaschewski, O. & Hesselmann, K., *Thermochemical Properties of Inorganic Substances*. Springer, 1991, pp. 1168–71.
15. Prasadarao, A. V., Selvaraj, U., Komarneni, S., Bhalla, A. S. & Roy, R., Enhanced densification by seeding of sol-gel-derived aluminum titanate. *J. Am. Ceram. Soc.*, **75** (1992) 1529–33.